The Egyptian Journal of Radiology and Nuclear Medicine 47 (2016) 1211–1220

Contents lists available at ScienceDirect

The Egyptian Journal of Radiology and Nuclear Medicine

journal homepage: www.sciencedirect.com/locate/ejrnm

Original Article

Benign versus malignant focal liver lesions: Diagnostic value of qualitative and quantitative diffusion weighted MR imaging

Nahla Mohamed Ali Hasan *, Khaled Fawzy Zaki, Mohamad Hasan Alam-Eldeen, Heba Rashdan Hamedi

Department of Diagnostic Radiology, Sohag Faculty of Medicine, Sohag University Hospital, Egypt

ARTICLE INFO

Article history:
Received 6 April 2016
Revised 5 August 2016
Accepted 8 August 2016
Available online 3 September 2016

Keywords:
Focal live lesions (FLLs)
Diffusion weighted imaging (DWI)
Apparent diffusion coefficient (ADC)

ABSTRACT

Background and objective: Diffusion-weighted imaging has an emerging role for assessment of focal and diffuse liver diseases. The aim of this study was to evaluate the diagnostic performance of DWI for characterization of focal liver lesions (FLLs).

Patients and methods: This prospective study included 40 consecutive patients with 64 focal liver lesions, who underwent MRI of the liver. All patients had one or more hepatic focal lesion of diameter more than 1 cm. DWI was reviewed (*b* values of 0, 50 and 600 s/mm^2) and the mean ADC was calculated.

Results: Quantitative assessment using ADC map was more accurate (87.5%) than qualitative assessment using DWI (75%) in characterization of FLLs. Mean ADC values of malignant lesions ($0.94 + 0.32 \times 10^{-3}$ mm^2/s) were significantly lower than those of benign lesions ($2.64 + 0.46 \times 10^{-3}$ mm^2/s), ($P < 0.001$). Using an ADC value above 1.6×10^{-3} mm^2/s offered the best accuracy in differentiation of malignant from benign lesions (86%).

Conclusion: DWI is a useful tool for FLLs characterization. Because of its known pitfalls and limitations, mainly the considerable overlap of ADCs values between solid benign and malignant lesions, it should be interpreted in combination with clinical data and conventional MRI sequences.

1. Introduction

Focal liver lesions (FLLs) are common in the general population. FLLs could be classified into 3 clinical categories: first, benign lesions for which no treatment is needed (hepatic hemangioma, focal nodular hyperplasia (FNH), benign liver cyst, and focal fat sparing); second, benign lesions for which treatment is required (hepatic adenoma, adenomatosis, biliary cystadenoma, hepatic abscess, echinococcal cyst, granulomatous inflammation and inflammatory psuedotumor of the liver); and third, malignant mass lesions for which treatment is always required if feasible (hepatocellular carcinoma (HCC), cholangiocarcinoma, liver metastases from other primary sites, biliary cystadenocarcinoma, hepatic angiosarcoma and lymphoma) [1].

Differentiation between malignant and benign FLLs and establishing the correct diagnosis are of great importance in treatment planning for patients with liver neoplasms and in patients without neoplasms for avoiding unnecessary liver biopsies.

Peer review under responsibility of The Egyptian Society of Radiology and Nuclear Medicine.

* Corresponding author. Fax: +20 93460296.
E-mail address: Nahla.hasan@ymail.com (N.M.A. Hasan).

http://dx.doi.org/10.1016/j.ejrnm.2016.08.009
0378-603X/

Imaging is an important decision-making tool in the diagnosis of FLLs as it can accurately differentiate benign from malignant lesions in most of the cases [2]. Ultrasound (US), computed tomography (CT) and magnetic resonance imaging (MRI) are the common modalities used. A meta-analysis study comparing contrast-enhanced ultrasound, CT, and MRI in evaluating incidental FLLs showed nearly similar diagnostic performance with specificities ranging from 82% to 89% without significant difference in the summary receiver operating characteristic curve (ROC) [3]. Because of the ionizing radiation of CT and relative non-availability of ultrasound contrast, MRI is considered the imaging modality of choice for FLL characterization. It relies on the signal characteristics of T1-weighted, T2-weighted, and dynamic gadolinium-enhanced T1-weighted imaging [4–6].

Diffusion weighted imaging (DWI) is a relatively recent imaging tool, which enables qualitative and quantitative assessment of tissue diffusivity without use of contrast agent.

The sensitivity of a DWI sequence is characterized by its *b*-value, which reflects the influence of the gradients in DWI. The higher the *b*-value, the more sensitive the sequence is to diffusion effects. DWI is performed with at least two *b*-values. Diffusion is quantitatively expressed in the apparent diffusion coefficient (ADC) which is related to the molecular mobility of water molecules and reflects tissue properties such as the size of the extracellular space, viscosity and cellularity. Low ADC values reflect restricted diffusion, and thus in highly cellular tissues. High ADC values denote areas with relative free diffusion, and thus in low cellular tissues [7,8].

With advances in hardware and coil systems, DWI has a high contrast resolution allowing accurate FLLs detection and characterization [9]. There are an increasing number of studies concerned about quantitative measurements of apparent diffusion coefficient (ADC) in liver lesions; however, many discrepancies were founded in the reported ADC values [10]. Thus, the purpose of this study was to evaluate the qualitative and quantitative diagnostic performance of DWI for characterization of FLLs and to reach the best ADC cutoff for distinction between malignant and benign lesions.

2. Patients and methods

This study included 40 non-consecutive patients, 26 males and 14 females, ranging in age from 20- to 85 years old (mean, 58 years), who underwent MR imaging of the liver in MRI unit in Diagnostic Radiology Department at Sohag University Hospital from April 2012 to April 2013. The inclusion criteria were Adult patients who had one or more FLLs with a diameter more than 1 cm. Exclusion criteria were as follows: patients under age of 18 years, patients had no FLLs or had FLLs with a diameter less than 1 cm or had previously treated lesions. Patients who did not undergo DWI nor had non-interpretable DWI sequences due to artifacts were also excluded.

Written consent was taken from the patients in accord with the ethics committee of our institution.

2.1. MRI protocol

All MRIs had been obtained by using 1.5-T machine (Philips- Acheiva), Netherlands. Sense flex coil was applied. Pulse sequences included axial breath-hold fast spine echo T2-weighted images (TR/ TE = 1852/70 ms, flip angle = 90°, field of view = 375 mm, slice thickness = 7 mm, with 0.7 mm intersection gap and matrix = 192 × 192), axial short tau inversion recovery (STIR) (TR/ TE = 669/70 ms, flip angle = 180°, field of view = 375 mm, slice thickness = 7 mm, with a 0.7 mm intersection gap and matrix = 192 × 192), axial dynamic T1-weighted fat-suppressed spoiled gradient-recalled-echo sequence, using magnifest 0.2 ml/kg body weight (TR/TE = 4.2/1.8 ms, flip angle = 15°, field of view = 375 mm, slice thickness = 7 mm, with 1 mm intersection gap and matrix = 175 × 256), respiratory-triggered axial fat-suppressed single-shot echo-planar DW imaging (TR/TE = 3000/100 ms, flip angle = 140°, field of view = 395 mm, slice thickness = 7 mm, with 0.7 mm intersection gap and matrix = 384 × 381), and DWI was obtained at different *b* values (0, 50 for FLLs detection], and 600 s/mm^2 [for FLLs characterization] within the same acquisition. Pixel-based ADC maps were reconstructed on the workstation. Three *b* values (0, 50, and 600 s/mm^2) were used for ADC calculation. The ADC value of each FLL was calculated within a region of interest (ROI) placed in the center of the assessed lesion, covering more than 50% of its surface. In cases of necrotic FLLs, measurements were taken only in the solid part, trying to avoid inclusion within the ROI of any necrotic part. Each lesion was individually analyzed in cases with multiple FLLs. Mean ADC measurement was calculated for each hepatic pathology.

2.2. Image analysis

The following data were recorded for each FLL: site, size, morphology, signal intensity of all used sequences (dynamic contrast material–enhanced T1WI, T2W FSE, STIR, DWI and ADC map).

The lesion was considered benign if it was hyperintense on DW images at $b = 0$ s/mm^2 and strongly decreased in signal intensity at $b = 600$ s/mm^2 and subjectively higher an ADC than that of the liver, apart from regeneration nodules (9 cases), those had low signal in T2WIs and hence low signal at $b = 0$, and $b = 600$, while the lesion was considered malignant if it was mildly to moderately hyperintense on DW images at $b = 0$ s/mm^2 and remained hyperintense at $b = 600$ s/mm^2 compared with liver parenchyma, with ADC signal lower than that of the liver parenchyma. If the above criteria were not obtained (e.g. isointense ADC or there was a partial signal intensity decrease), the lesion was considered indeterminate [11–13].

Our standard of reference was based on the histopathological findings in 21 patients (9 HCCs, 5 metastatic lesions, 3 cholangiocarcinomas, 2 liver abscesses, one intra hepatic hematoma, and one FNH). Diagnosis of the remaining 19 cases was based on clinical data, typical MR imaging findings (T2-weighted, and dynamic contrast material–enhanced T1-weighted images), findings of other imaging

modalities (CT and U/S), and clinical and imaging follow-up results.

2.3. Statistical analysis

Descriptive analyses of demographic, clinical, radiological, and pathological characteristics were done. The variables studied were described with mean ± standard deviation to measure the degree of dispersion of data around their mean. T-student test was applied to test the presence of significant differences between two comparable qualitative variables (benign versus malignant), depending on the features assessed. The receiver operating characteristic curve was constructed and its parameters (sensitivity, specificity, positive predictive value, and negative predictive value) as well as the accuracy for each ADC threshold were estimated to identify the best ADC value to distinguish between benign and malignant FLLs.

SPSS statistical software was used with *P* value less than 0.05 was considered to indicate a significant difference.

4. Results

A total of 40 consecutive adult patients had 64 HFLs with an average diameter of 3.4 cm (range from 1.2 to 14 cm) met all of the inclusion criteria, 26 males (65%) and 14 females (35%), ranging in age from 20 to 85 years old (mean, 58 years). Twenty-four patients (60%) presented with 36 malignant liver lesions; 20 metastases, 13 hepatocellular carcinomas (Fig. 1) and 3 Cholangiocarcinomas (Fig. 2) and sixteen patients (40%) presented with 28 benign liver lesions; 12 hemangiomas (Fig. 3), 9 regenerating nodules, 3 cysts (Fig. 4), 2 abscesses (Fig. 5), 1 focal nodular hyperplasia (Fig. 6) and 1 hematoma. The average number of FLLs/patient was 1.6. None of the patients simultaneously had benign and malignant liver lesions.

12 patients had a history of chronic liver disease (5 chronic hepatitis and 7 liver cirrhosis) and 6 patients had history of primary malignancy (2 cancer breast, 2 renal cell carcinoma, one cancer bladder (Fig. 7) and one lymphoma (Fig. 8). The remaining 22 patients, who had no history of malignancy or chronic liver disease, underwent MR imaging for further evaluation of FLLs diagnosed by CT and or US.

Analysis of signal intensity on the *b*-600 showed statistically significant difference between benign and malignant FLLs (p value <0.001) with sensitivity and specificity of hyperintensity for malignant FLLs were 91.7% and 53.5% respectively while decreased hyperintensity showed sensitivity and specificity for benign FLLs of 83.3% and 71.1% respectively. The overall accuracy of qualitative DW images for FLLs characterization was 75% (48 of 64) Table 1.

Analysis of signal intensity on the ADC map showed that hypointensity on ADC map is 100% specific for malignant FLLs diagnosis. On the other hand specificity of hyperintensity on the ADC map for benign FLLs was 97.2%. The overall accuracy of ADC map in FLLs characterization was 87.5% Table 2.

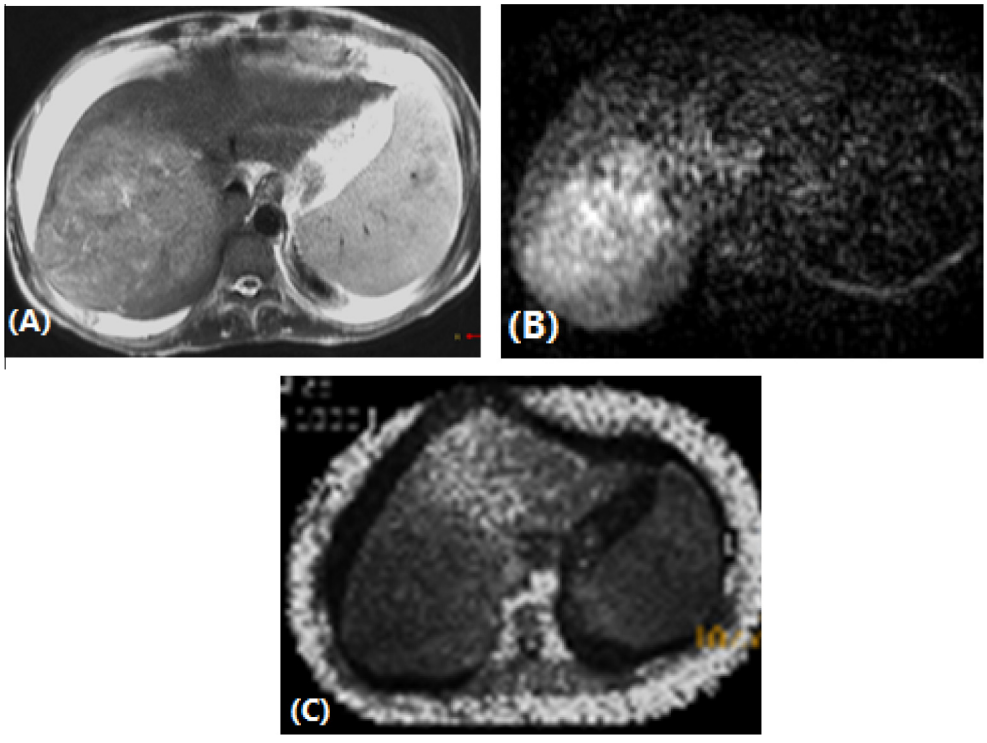

Fig. 1. HCC in liver cirrhosis in a 45 year-old female patient. (A) Axial T2-weighted image shows moderately hyperintense right lobe large lesion. Note the associated ascites. (B) DWI ($b = 600$) image shows the hyperintensity of the lesion. (C) ADC map shows hypointense lesion with low ADC value (0.98×10^{-3}mm^2/s).

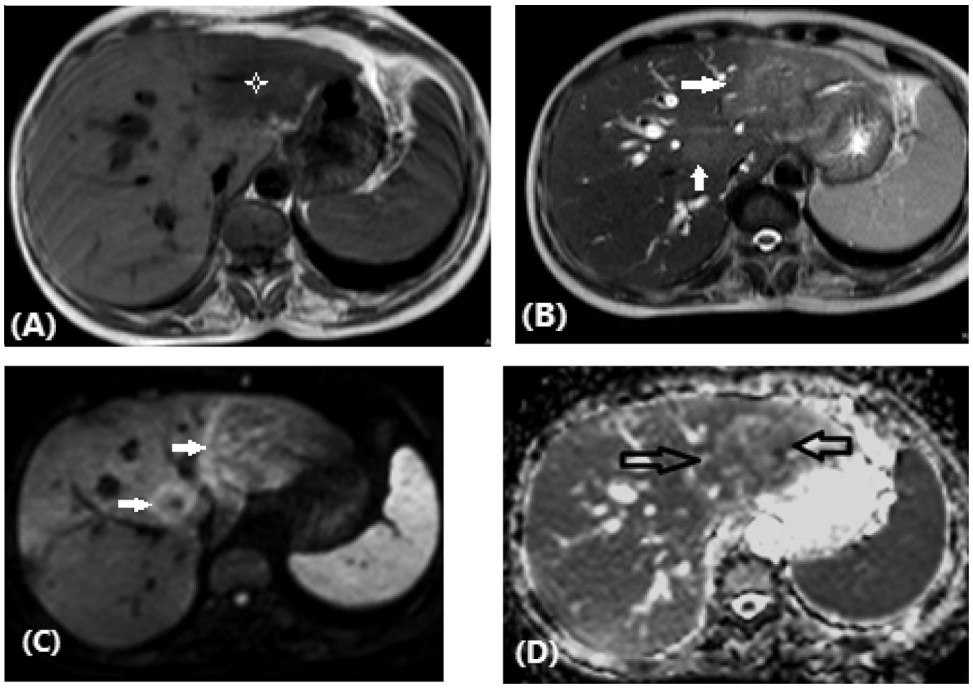

Fig. 2. Cholangiocarcinoma in a 55 year-old female patient. (A) Axial T1-weighted image displays an ill-defined hypointense lesion (asterisk) within the left lobe. (B) Axial T2-weighted image, the lesion is slightly hyperintense (arrows). (C) DWI (b = 600) image shows peripheral rim of hyperintensity, giving rise to a "target-sign"(arrows). (D) On the ADC map, the lesion is isointense (arrows) with low ADC value (0.93×10^{-3}mm^2/s).

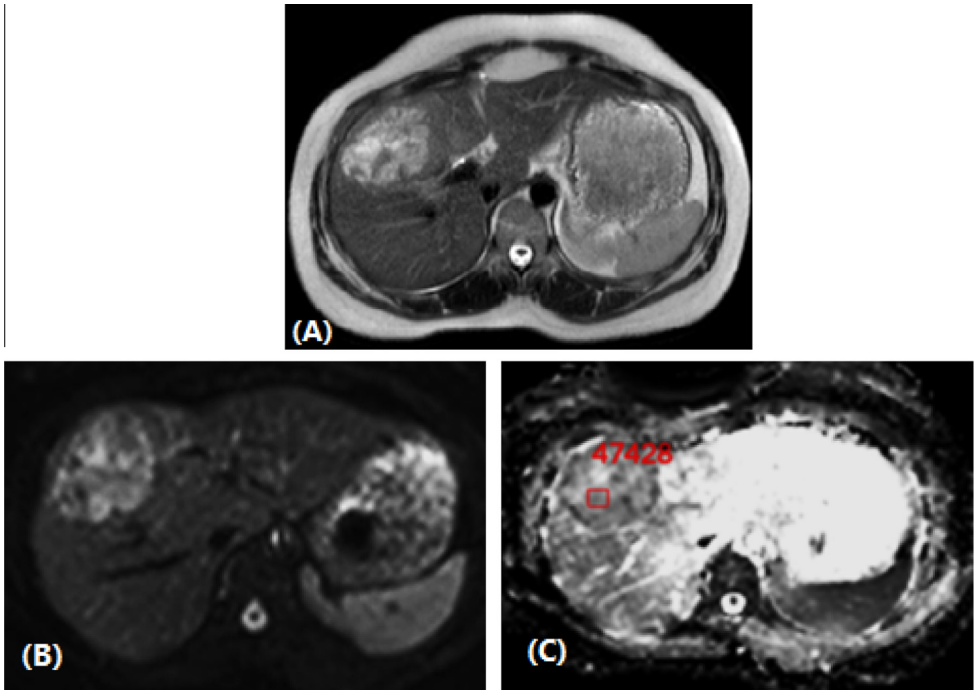

Fig. 3. Liver hemangioma in a 38 year-old female patient. (A) Axial T2-weighted image discloses a lobulated hyperintense lesion in the right lobe. (B) Axial single-shot echo-planar DW image (b = 600), the hemangioma persists with high signal intensity (tissue with greater cellularity/T2 shine-through). (C) The ADC map shows the lesion is isointense with a high ADC value (3.8×10^{-3} mm^2/s).

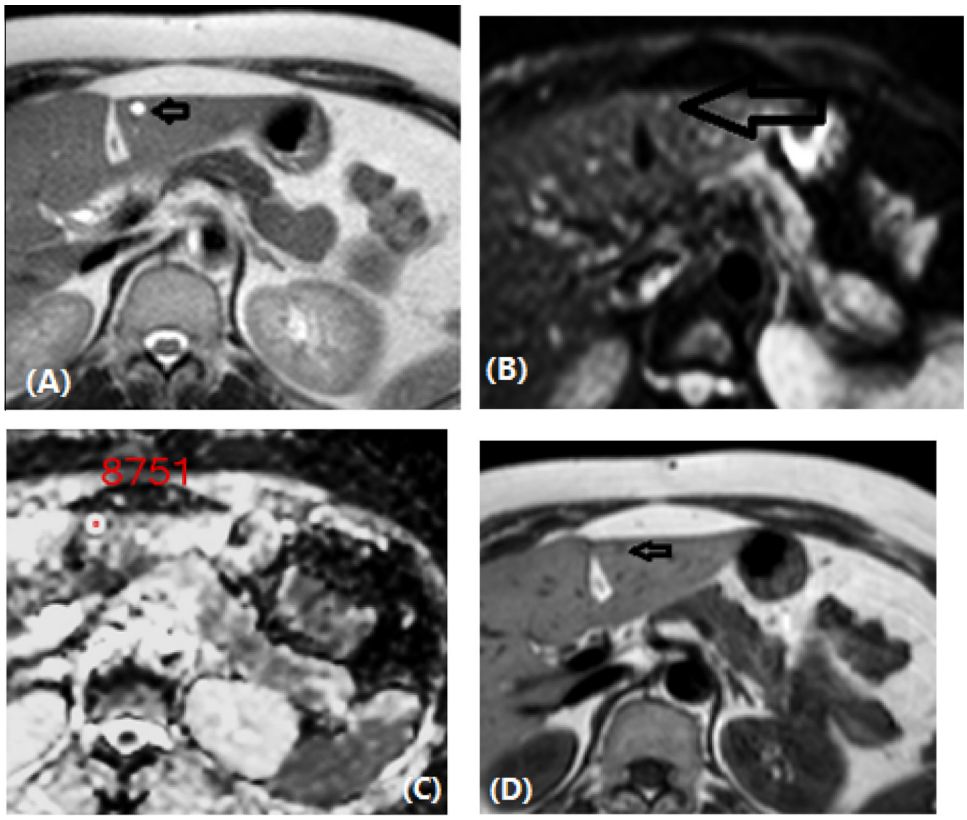

Fig. 4. Hepatic small simple cyst in a 45 year-old female patient. (A) Axial T2-weighted image discloses a tinny hyperintense lesion in the left lobe (arrow). (B) Axial single-shot echo-planar DW image ($b = 600$), the lesion shows T2 shine-through rather than restricted diffusion (some signal loss occurring) (arrow). (C) On the ADC map, the lesion is markedly hyperintense with high ADC value (3.1×10^{-3} mm^2/s) (asterisk). (D) Axial T1-weighted image, the hypointense left hepatic lobe cyst (arrow) is more difficult to see.

Mean ADC values of all included FLLs were reflected in Table 3. Mean ADC values of malignant lesions ($0.94 \pm 0.32 \times 10^{-3}$ mm^2/s) were significantly lower than those of benign lesions ($2.64 \pm 0.46 \times 10^{-3}$ mm^2/s) with a significant overlap (Fig. 9).

Using 1.05 as a cutoff ADC value led to a sensitivity for malignancy of 63.9% and specificity of 96.4% with 78.1% accuracy. Using a higher ADC value, such as 1.6, the sensitivity and specificity for malignancy were 100% and 67.9% respectively with 86% accuracy and 100% negative predictive value Table 4.

5. Discussion

Most of liver masses arising in noncirrhotic livers are benign. The most common solid benign lesions are hemangiomas, adenomas, and FNH [14,15], while metastases are the most commonly encountered malignant lesions [3]. HCC and intrahepatic cholangiocarcinoma occur in the setting of chronic liver disease [16].

In most cases, the differential diagnosis of FLLs is straightforward, as the majority of FLLs have a characteristic imaging aspect allowing a confident final diagnosis; however, imaging diagnosis of atypical FLL is difficult, and follow-up and/or biopsy are often required [2].

MRI is the imaging test of choice for liver-mass characterization, demonstrating similar if not superior performance to CT. DWI plays an emerging role for the assessment of focal and diffuse liver diseases. DWI can be easily included in routine liver MRI protocols, as it takes a short time as two breathhold acquisitions and non-contrast technique; so, it can be done for patients with severe renal insufficiency, at risk for nephrogenic systemic fibrosis [9]. DWI is a measure of the ability of water molecule protons to diffuse freely within intra- and extracellular environments. Therefore, DWI of FLL denotes cellular density of the lesion, while ADC values are quantifiable measures reflecting both diffusion and perfusion within imaged tissue [16].

In the present study, qualitative (signal intensity on DW images and ADC map) and quantitative (ADC value) were used to differentiate between benign and malignant FLLs. In accordance with the previous literature [11–13], we used b value of 0, 50 and 600 s/mm^2 for visual discrimination between benign and malignant FLLs, on the basis of lesion morphology, signal intensity and degree of signal intensity decrease with increasing b values, and it showed 75% overall accuracy for FLLs characterization compared with 89.1% reported by Parikh et al. in their study [17]. The lower percentage of our results could be a result of

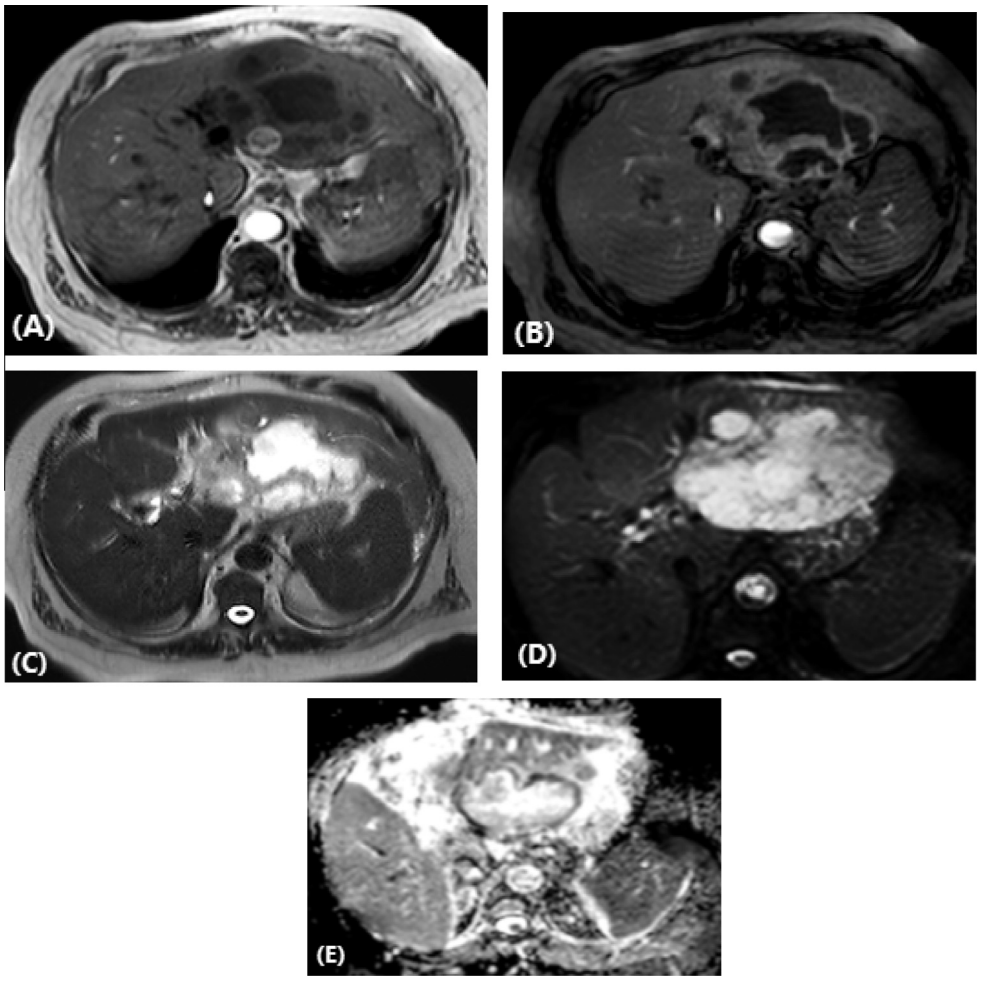

Fig. 5. Liver abscess in a 72 year-old male patient. (A) Axial T1-weighted image shows a multiloculated hypointense cystic lesion in the left lobe. (B) Axial T1-weighted image following intravenous contrast injection at the same level of (A) and shows intense marginal enhancement. (C) Axial T2-weighted image discloses a hyperintense abscess cavity. (D) Axial single-shot echo-planar DW image ($b = 600$), the abscess persists with high signal intensity with ADC value [1.7×10^{-3}mm^2/s] (E).

the common pitfalls of DWI including slow-flowing blood in hemangioma that is responsible for its high signal intensity on *b* value 600 and consequently it could be mistaken for malignant lesion [18], and T2 shine-through phenomenon that was encountered in 11 (39.3%) benign FLLs on *b* value 600.

T2 shine-through phenomenon describes a lesion that shows restricted diffusion on DWI because of the long T2-relaxation time rather than the limited mobility of the water protons. The presence of T2 shine-through is known by correlation of high- *b* –value images with the ADC map. Areas demonstrating mainly T2 shine-through rather than restricted diffusion have high diffusivity on the ADC map and high ADC values [19], as it was confirmed in our results with increased overall accuracy for FLLs characterization on ADC map up to 87.5%. Therefore, DW images should be interpreted in combination with the ADC map and conventional MRI sequences to avoid misinterpretation.

Several studies have been suggested that ADC values can discriminate between benign and malignant focal liver lesions [20–25], but many discrepancies in the reported ADC values were encountered. This is mainly because of using different techniques, scanning parameters and different *b*-values [21], in addition to the different liver lesions assessed.

In accordance with the more performed techniques in previous studies, 0, 50 and 600 s/mm^2 *b* values were used in the present study to calculate the ADC values and images were obtained using triggered breathing.

In general, malignant FLLs have ADC values lower than those of benign lesions, with overlap of variable degrees [19]. Lower ADC values for most malignant lesions are thought to be due to cellular membranes impeding the water molecules mobility. However, solid benign lesions with high cellularity also have low ADC values. On the other hand, cystic and necrotic malignant lesions exhibit high ADC values as a result of larger diffusion distances caused by lost membrane integrity [21].

In the current study, Mean ADC values of malignant lesions ($0.94 \pm 0.32 \times 10^{-3}$ mm^2/s) were significantly

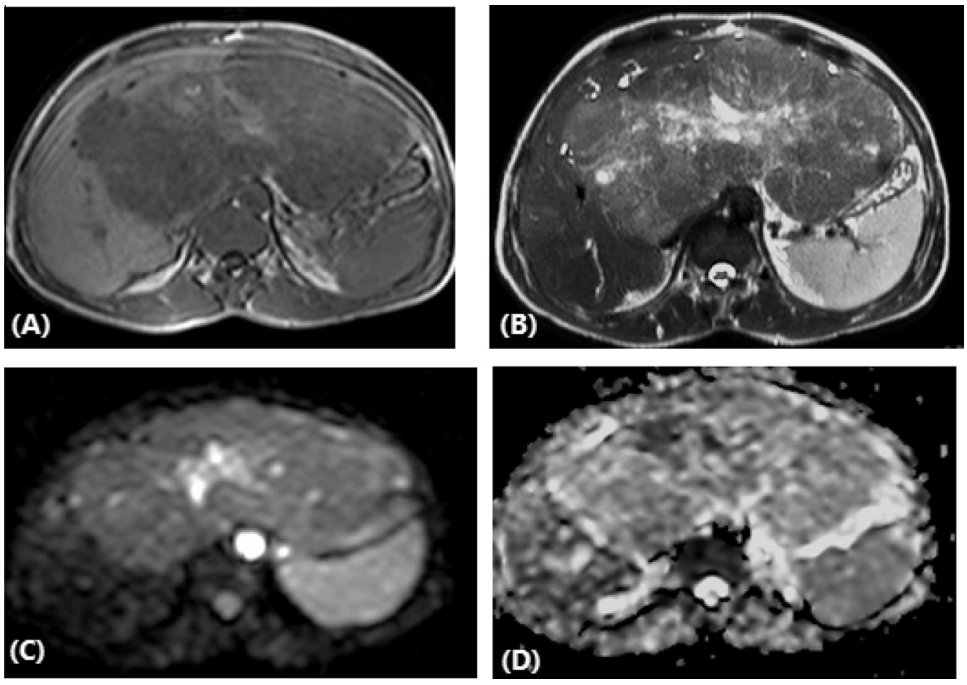

Fig. 6. FNH in a 59 year-old female patient; (A) Axial T1-weighted image displays a well-defined large hypointense lesion within the left lobe. (B) Axial T2-weighted image discloses T2 iso/hyperintense lesion with central markedly hyperintense scar, consistent with focal nodular hyperplasia. (C) Axial single-shot echo-planar DW image ($b = 600$), the FNH is moderately hyperintense with more hyperintense central scar (D) On the ADC map, the lesion is isointense with a relatively low ADC value (1.4×10^{-3}mm^2/s).

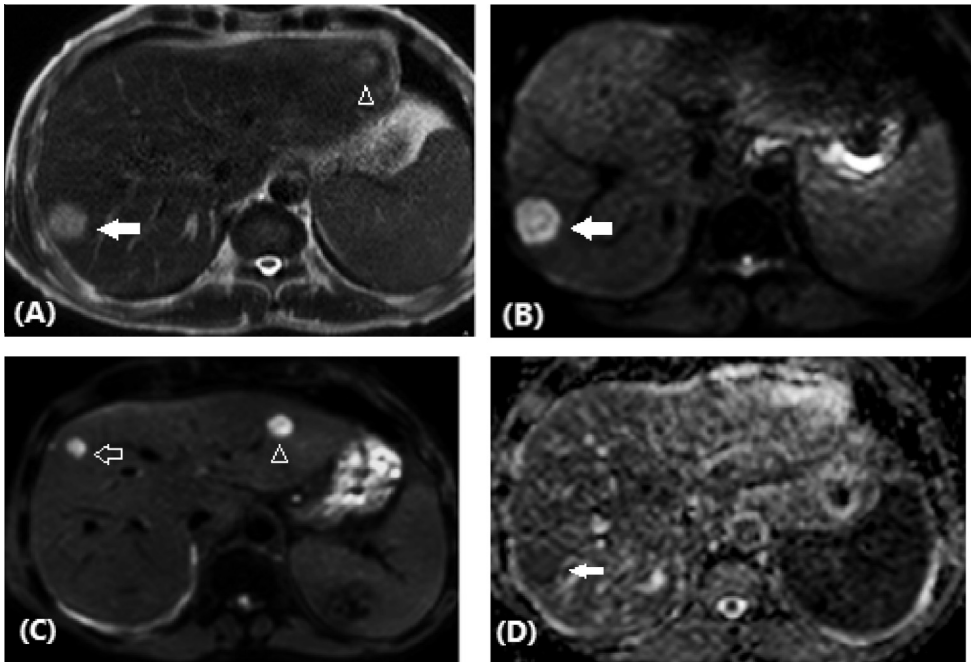

Fig. 7. Hepatic metastasis from cancer bladder in a 70 year-old male patient. (A) Axial fat suppressed T2-weighted image displays moderately hyperintense right lobe focal lesion (arrow) and another ill-defined less bright left lobe lesion (arrow head). (B) & (C) DWI ($b = 600$) images shows three markedly hyperintense lesions. (D) On the ADC map at A and B levels, the right lobe lesion is hypointense (arrow) with low ADC value (1.3×10^{-3} mm^2/s).

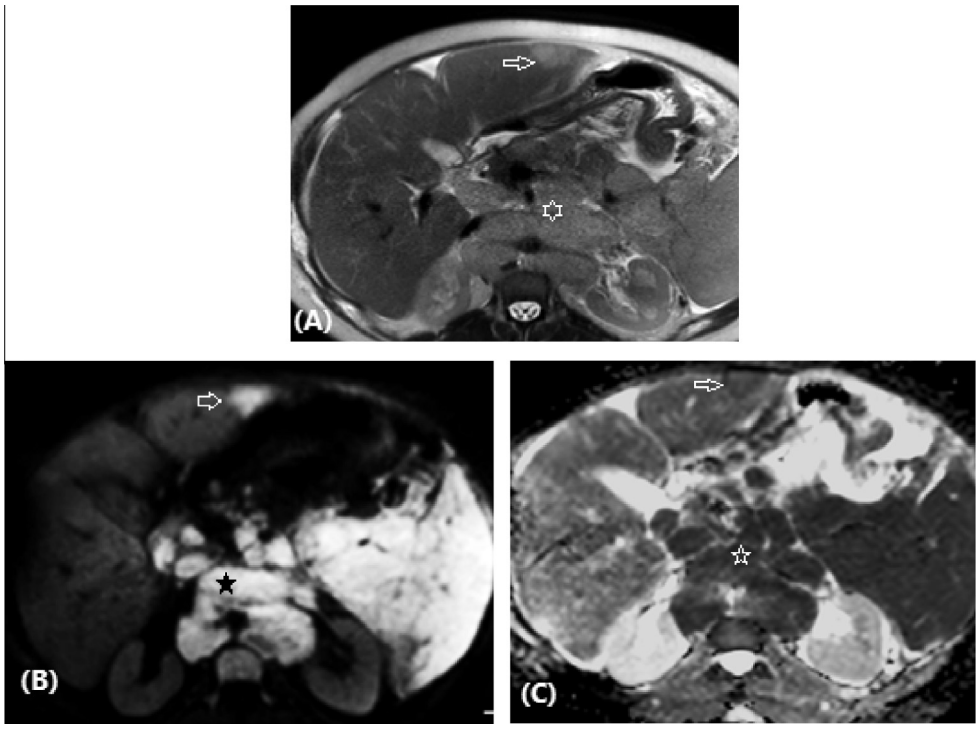

Fig. 8. Lymphoma in a 28 year-old female patient (A) Axial T2-weighted image displays an ill-defined slight hyperintense left lobe focal lesion (arrow). Note the associated multiple enlarged paraortic and porta hepatis lymph nodes (asterisk). (B) DWI (b = 600) image shows obviously the hyperintense hepatic lesion (arrow) and the enlarged lymph nodes (asterisk). (C) On the ADC map, both hepatic lesion (arrow) and lymph nodes (asterisk) are hypointense with low ADC value (1.1×10^{-3} mm^2/s).

Table 1
Signal intensity and accuracy of DWI at b value-600 for differentiation between benign and malignant focal liver lesions.

Lesion type	Signal intensity at b value-600 s/mm^2		Total (%)	P value	Overall accuracy (%)
	Hyperintense (%)	Decreased hyperintensity (%)			
Benign HFLs	13 (46.4)	15 (53.6)	28 (100)	<0.001	86
Malignant HFLs	33 (91.7)	3 (8.3)	36 (100)		

* P value is highly significance (<0.001).

Table 2
Signal intensity and accuracy of ADC map for differentiation between benign and malignant focal liver lesions.

Lesion type	Signal intensity on ADC map			Total (%)	P value	Overall accuracy (%)
	Hyperintense (%)	Isointense (%)	Hypointense (%)			
Benign HFLs	26 (93)	2 (7)	0 (0)	28 (100)	<0.001	87.5
Malignant HFLs	1 (2.8)	5 (13.9)	30 (83.3)	36 (100)		

* P value is highly significance (<0.001).

lower than those of benign lesions ($2.64 \pm 0.46 \times 10^{-3}$ mm^2/s) with overlap in-between.

As the most challenging task in FLLs diagnosis is to differentiate between malignant and benign solid liver tumors, detection of the best ADC cutoff value and its accuracy to distinguish malignant and solid benign liver lesions are valuable.

Different ADC cutoffs ($1.4–1.6 \times 10^{-3}$ mm^2/s) have been reported in previous studies, with a sensitivity ranged from 74% to 100% and specificity ranged from 77% to 100% for diagnosing malignant lesions [11,17,20,26–28]. However, the specificity decreased by exclusion of cysts and hemangiomas, suggesting that the ADC cutoff is not as effective in differentiation of malignant lesions from FNHs, adenomas, or abscesses.

Our results reported accuracy of ADC cutoff for the diagnosis of malignant focal lesions, ranged from 78.1% to 86% depending on ADC threshold used. Using ADC cutoff of

Table 3
Distribution and mean ADC values for benign and malignant focal liver lesions.

Lesion type	Number of patients (%)	Number of lesions (%)	ADC value
Benign HFLs	16 (40)	28 (43.75)	(0.67–5) 2.64 ± 0.46
Hemangioma	5 (12.5)	12 (18.75)	(1.23–3.91) 3.36 ± 0.26
Regenerating Nodule	5 (12.5)	9 (14)	(0.67–1.47) 0.88 ± 0.37
Abscess	2 (5)	3 (4.7)	(1.6–4.21) 3.45 ± 0.64
Cyst	2 (5)	2 (3.1)	(3–4.7) 3.85 ± 0.57
FNH	1 (2.5)	1 (1.6)	1.4 ± 0.4
Hematoma	1 (2.5)	1 (1.6)	5 ± 0.12
Malignant HFLs	24 (60)	36 (56.25)	(0.54–1.6) 0.94 ± 0.32
HCC	12 (30)	13 (20.3)	(0.78–1.6) 0.93 ± 0.37
Metastases	9 (22.5)	20 (31.25)	(0.34–1.23) 0.89 ± 0.25
Cholangiocarcinoma	3 (7.5)	3 (4.7)	(0.96–1.2) 1.13 ± 0.21

Note: *HCC*; Hepatocellular carcinoma, *FNH*; Focal nodular hyperplasia, ADC values are expressed as the lowest, highest and (mean) ADC values ± Standard deviation.

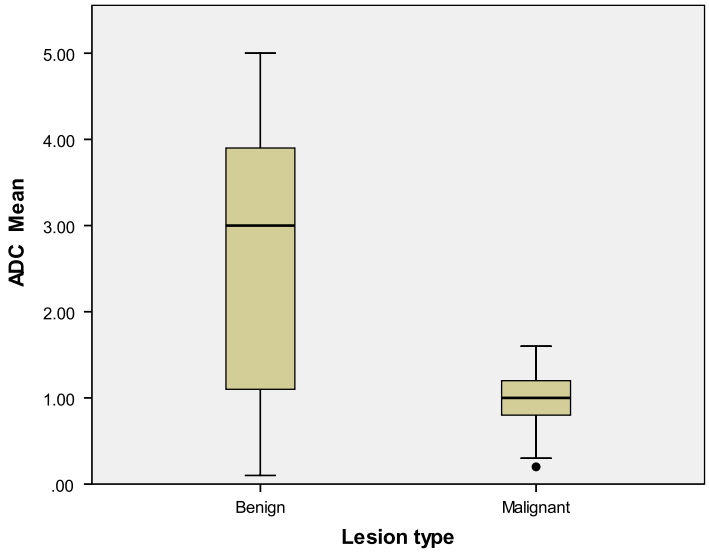

Fig. 9. Box plot illustrating mean ADC values for benign and malignant HFLs.

Table 4
Diagnostic value of different ADC thresholds for Diagnosing Malignant FLLs.

ADC threshold	Sensitivity (%)	Specificity (%)	PPV (%)	NPV (%)	Accuracy (%)
1.6	100	68	80	100	86
1.2	83.3	85.7	88.2	80	84.4
1.05	63.9	96.4	95.8	67.5	78.1

* *P* value is highly significance (<0.001).

1.6×10^{-3} mm^2/s led to the highest accuracy for the differentiation of malignant and benign liver lesions (86%) with a sensitivity of 100% and a specificity of 68% for malignant lesions. Its strength was in its 100% negative predictive value where ADC values above 1.6×10^{-3} mm^2/s exclude the malignant lesions. However, the relatively lower specificity compared with those of the literature could be explained by inclusion of regenerating nodules (9 out of 28 benign lesions) in our series with a mean ADC value of $0.88 \pm 0.37 \times 10^{-3}$ mm^2/s which is parallel to that of malignant lesions.

By comparing our ADC cutoff with the literature, differences in sensitivity and specificity and accuracy are small. The only study with significantly different results from ours included 38 patients presented with 37 FLLs and 68% of the benign lesions were biliary cysts with significantly higher ADC value than other lesions [20].

Some potential limitations are encountered in this study; first is the limited image quality of single shot SE echo-planar DW MR imaging, including low spatial resolution, poor SNR, and echo-planar imaging–related artifacts. Second, the small number of patients relative to the high

variability in pathology included, lack of cases of adenomas and only one case of FNH was included. Third, the unavailable histopathological findings in some cases (19 [47.5%] cases).

6. Conclusion

DWI is a useful tool for FLLs characterization. Qualitative DWI assessment is not sufficient alone and should be combined with quantitative ADC value calculation. DWI should be included in routine liver MR protocols, however, because of its known pitfalls and limitations, mainly the substantial overlap in the range of ADCs between solid benign and malignant lesions, it should be interpreted in combination with clinical history and conventional sequences including contrast enhanced MRI.

Conflict of interest

The authors declare that there are no conflict of interests.

References

[1] Roberts LR. Clinical approach to liver mass lesions. In: Hauser SC, editor. Mayo clinic gastroenterology and hepatology board review. New York, NY: Mayo Clinic Scientific Press: Oxford University Press; 2011. p. 281–94.
[2] Caraiani C, Chiorean L, Fenesan D, Lebovici A, Feier D, Gersak M, et al. Diffusion weighted magnetic resonance imaging for the classification of focal liver lesions as benign or malignant. J Gastrointestin Liver Dis 2015;3(24):309–17.
[3] Xie L, Guang Y, Ding H, Cai A, Huang Y. Diagnostic value of contrast-enhanced ultrasound, computed tomography and magnetic resonance imaging for focal liver lesions: a meta-analysis. Ultrasound Med Biol 2011;37:854–61.
[4] Hussain SM, Semelka RC, Mitchell DG. MR imaging of hepatocellular carcinoma. Magn Reson Imag Clin N Am 2002;10:31–52.
[5] Pedro MS, Semelka RC, Braga L. MR imaging of hepatic metastases. Magn Reson Imaging Clin N Am 2002;10:15–29.
[6] Motohara T, Semelka RC, Nagase L. MR imaging of benign hepatic tumors. Magn Reson Imaging Clin N Am 2002;10:1–14.
[7] Bammer R. Basic principles of diffusion-weighted imaging. Eur J Radiol 2003;45:169–84.
[8] Kwee TC, Takahara T, Ochiai R, Nievelstein RA, Luijten PR. Diffusion-weighted whole-body imaging with background body signal suppression (DWIBS): features and potential applications in oncology. Eur Radiol 2008;18:1937–52.
[9] Galea N, Cantisani V, Taouli B. Liver lesion detection and characterization: role of diffusion-weighted imaging. J Magn Reson Imaging 2013;37:1260–76.
[10] Kele PG, Jagt EJ. Diffusion weighted imaging in the liver. World J Gastroenterol 2010;16(13):1567–76.
[11] Taouli B, Vilgrain V, Dumont E, Daire JL, Fan B, Menu Y. Evaluation of liver diffusion isotropy and characterization of focal hepatic lesions with two single-shot echoplanar MR imaging sequences: prospective study in 66 patients. Radiology 2003;226:71–8.
[12] Krinsky GA, Lee VS, Theise ND, et al. Hepatocellular carcinoma and dysplastic nodules in patients with cirrhosis: prospective diagnosis with MR imaging and explantation correlation. Radiology 2001;219:445–54.
[13] Danet IM, Semelka RC, Leonardou P, et al. Spectrum of MRI appearances of untreated metastases of the liver. AJR Am J Roentgenol 2003;181:809–17.
[14] Craig J, Peters R, Edmondson H. Tumors of the liver and intrahepatic bile ducts. In: Hartman H, Sobin L, editors. Atlas of Tumor Pathology. 2nd series, fascicle 26. Washington, DC: Armed Forces Institute of Pathology,; 1989.
[15] Karhunen PJ. Benign hepatic tumours and tumour like conditions in men. J Clin Pathol 1986;39:183–8.
[16] Fowler KJ, Brown JJ, Narra VR. Magnetic resonance imaging of focal liver lesions: approach to imaging diagnosis. Hepatology 2011;54:2227–37.
[17] Parikh T, Drew SJ, Lee VS, Wong S, Hecht EM, Babb JS, et al. Focal liver lesion detection and characterization with diffusion weighted mr imaging: comparison with standard breath-hold T2-weighted imaging. Radiology 2008;3(246):812–22.
[18] Qayyum A. Diffusion-weighted Imaging in the Abdomen and Pelvis: concepts and applications. RadioGraphics 2009;29:1797–810.
[19] Taouli B, Koh D. Diffusion-weighted MR imaging of the liver. Radiology 2010;254(1):47–66.
[20] Gourtsoyianni S, Papanikolaou N, Yarmenitis S, Maris T, Karantanas A, Gourtsoyiannis N. Respiratory gated diffusion-weighted imaging of the liver: value of apparent diffusion coefficient measurements in the differentiation between most commonly encountered benign and malignant focal liver lesions. Eur Radiol 2008;18:486–92.
[21] Goshima S, Kanematsu M, Kondo H, Yokoyama R, Kajita K, Tsuge Y, et al. Diffusion-weighted imaging of the liver: optimizing b value for the detection and characterization of benign and malignant hepatic lesions. J Magn Reson Imag 2008;28:691–7.
[22] Feuerlein S, Pauls S, Juchems MS, Stuber T, Hoffmann MH, Brambs HJ, et al. Pitfalls in abdominal diffusion-weighted imaging: how predictive is restricted water diffusion for malignancy. AJR Am J Roentgenol 2009;193:1070–6.
[23] Sandrasegaran K, Akisik FM, Lin C, Tahir B, Rajan J, Aisen AM. The value of diffusion-weighted imaging in characterizing focal liver masses. Acad Radiol 2009;16:1208–14.
[24] Kandpal H, Sharma R, Madhusudhan KS, Kapoor KS. Respiratory-triggered versus breath-hold diffusion-weighted MRI of liver lesions: comparison of image quality and apparent diffusion coefficient values. AJR Am J Roentgenol 2009;192:915–22.
[25] Coenegrachts K, Matos C, ter Beek L, Metens T, Haspeslagh M, Bipat S, et al. Focal liver lesion detection and characterization: comparison of non-contrast enhanced and SPIO-enhanced diffusion-weighted single-shot spin echo echo planar and turbo spin echo T2-weighted imaging. Eur J Radiol 2009;72:432–9.
[26] Bruegel M, Holzapfel K, Gaa J, et al. Characterization of focal liver lesions by ADC measurements using a respiratory triggered diffusion-weighted single-shot echo-planar MR imaging technique. Eur Radiol 2008;18:477–85.
[27] Namimoto T, Yamashita Y, Sumi S, Tang Y, Takahashi M. Focal liver masses: characterization with diffusion-weighted echo-planar MR imaging. Radiology 1997;204:739–44.
[28] Kim T, Murakami T, Takahashi S, Hori M, Tsuda K, Nakamura H. Diffusion-weighted single-shot echoplanar MR imaging for liver disease. AJR Am J Roentgenol 1999;173:393–8.